Distance measurements using paramagnetic ion-induced relaxation in the saturation transfer electron spin resonance of spin-labeled biomolecules

Application to phospholipid bilayers and interdigitated gel phases

Tibor Páli, Rosa Bartucci, László I. Horváth, and Derek Marsh
Max-Planck-Institut für biophysikalische Chemie, Abteilung Spektroskopie, D-3400 Göttingen, Germany

ABSTRACT The saturation transfer electron spin resonance (STESR) spectra of spin-labeled phosphatidylcholines in gel phase lipid bilayers are shown to be sensitive to dipolar spin–spin interactions with paramagnetic ions in the aqueous phase. The reciprocal integrated intensity of the STESR spectrum is linearly dependent on aqueous Ni^{2+} ion concentration, hence, confirming the expectation that the STESR intensity is directly proportional to the spin-lattice relaxation time of the spin label. The gradient of the relaxation rate with respect to Ni^{2+} ion concentration decreases strongly with the position of the nitroxide group down the *sn*-2 chain of the spin-labeled lipid and is consistent with a $1/R^3$ dependence on the distance, R, from the bilayer surface. The values derived for the dimensions of the bilayer and lipid molecules in the case of dipalmitoyl phosphatidylcholine (DPPC) are in good agreement with those available from x-ray diffraction studies. Allowance for the multibilayer nature of the DPPC dispersions gives an estimate of the water layer thickness that is also consistent with results from x-ray diffraction. The profile of the paramagnetic ion-induced relaxation is drastically changed with DPPC dispersions in glycerol for which the lipid chains are known to be interdigitated in the gel phase. The terminal methyl groups of the lipid chains are located approximately in register with the C-3 atoms of the *sn*-2 chain of the oppositely oriented lipid molecules in the interdigitated phase. The thickness of the lipid layer and the effective thickness of the lipid polar group are reduced by ~40% in the interdigitated phase as compared with the bilayer phase. The calibrations of the distance dependence established by use of spin labels at defined chain positions should be applicable to STESR measurements on other biological systems.

INTRODUCTION

In addition to its well-established use for the study of slow rotational motion of spin-labeled biomolecules (Thomas et al., 1976), saturation transfer electron spin resonance (STESR)[1] spectroscopy has recently been shown to be sensitive to spin–spin interactions (Horváth et al., 1990; Marsh and Horváth, 1992). Effectively, saturation of a given spin packet can be alleviated by spin–spin interactions and this manifests itself in the STESR spectrum as a reduction in overall intensity, because the latter has been shown by spectral simulations to be approximately proportional to the spin-lattice relaxation time, T_1, of the spin label (Thomas et al., 1976). The sensitivity to the interaction is greater than that of conventional ESR and therefore, STESR is more suitable for the study of weak spin–spin interactions such as are likely to be encountered often in biological systems. So far, this newer aspect of the STESR method has been applied primarily to the study of Heisenberg spin exchange interactions (Marsh and Horváth, 1992; Khramtsov and Marsh, 1991; Fajer et al., 1992); the application to dipolar interactions remains yet to be explored.

Paramagnetic ions, which generally have short spin-lattice relaxation times, are known to relax efficiently the spins of nitroxide ESR labels by means of a dipolar mechanism (Likhtenshtein, 1976). Because the paramagnetic ion-induced relaxation depends very steeply on the separation of the dipoles, this provides a sensitive method for measuring distances on the molecular scale. Implementation of such measurements has been confined mostly to continuous wave saturation studies (Likhtenshtein, 1976, 1990; Hyde et al., 1979). In principle, STESR spectroscopy also has the potential for obtaining distance information via the dependence of the spectral intensity on the spin-lattice relaxation time of the spin label. The method has the advantage of simplicity and ease of use, if its reliability can be

Address correspondence to Dr. Marsh.

Dr. Páli's permanent address is Institute of Biophysics, Biological Research Center, Hungarian Academy of Sciences, P.O. Box 521, H-6071, Szeged, Hungary.

Dr. Bartucci's permanent address is Department of Physics, University of Calabria, I-87036 Arcavacata di Rende, Italy.

[1] *Abbreviations used in this paper:* DPPC, 1,2-dipalmitoyl-*sn*-glycero-3-phosphocholine; *n*-SASL, *n*-(4,4-dimethyloxazolidine-*N*-oxyl)stearic acid; *n*-PCSL, 1-acyl-2-[*n*-(4,4-dimethyloxazolidine-*N*-oxyl)stearoyl]-*sn*-glycero-3-phosphocholine; ESR, electron spin resonance; STESR, saturation transfer ESR; V_1, first harmonic ESR absorption signal detected in phase with respect to the field modulation; V_2, second harmonic absorption ESR signal detected 90° out-of-phase with respect to the field modulation.

0006-3495/92/06/1595/08 $2.00

established and suitable calibrations can be obtained on model systems.

In the present paper we study the paramagnetic effects of Ni^{2+} ions in the aqueous phase on the STESR spectra of phospholipid probes which are spin-labeled at different positions in the fatty acyl chain and are incorporated in bilayer model membranes. The dependence of the spectral intensity on the Ni^{2+} ion concentration is used to verify the proportionality with the spin label T_1. By working with gel phase lipid bilayers in which the lipid chains are extended in their all-*trans* configuration it is possible to calibrate the paramagnetic ion-induced changes in STESR integral intensity in terms of the known separation between the different labeling positions in the lipid chain. Bilayer and lipid polar group dimensions derived in this way are then checked against the corresponding values obtained from x-ray diffraction. The sensitivity of the method to the distance of closest approach between paramagnetic ion and spin label is used also to study the structural details of the lipid surface in a lipid gel phase in which interdigitation of the chains is induced by glycerol.

MATERIALS AND METHODS

Materials

Dipalmitoyl phosphatidylcholine (DPPC) was obtained from Fluka (Buchs, Switzerland) and the purity was checked by thin layer chromatography. The spin-labeled phosphatidylcholine derivatives (*n*-PCSL) were synthesized from the corresponding spin-labeled stearic acid analogues (*n*-SASL) as described in Marsh and Watts (1982). The purity of the spin-labeled phospholipids was checked by thin layer chromatography. Glycerol was from Merck (Darmstadt, Germany). Other chemicals used were of analytical grade purity.

Sample preparation

DPPC and spin-labeled lipid were codissolved at a mole ratio of 200–250:1 in dichloromethane and the solvent was then evaporated under nitrogen. The dry mixture was kept under vacuum overnight and was dispersed at a concentration of 0.1 mg/ml in argon-saturated double-distilled water, containing the desired concentration of $NiCl_2$, by vortex mixing at 60°C for 30 min. Samples in glycerol were prepared similarly by adding 25 μl of glycerol/$NiCl_2$ solution to 1 mg of the dry DPPC/spin label mixture. Aliquots of the lipid suspensions were loaded into 100 μl, 1-mm diameter glass capillaries flushed with argon and were centrifuged at 2,500 rpm for 10 min in a bench centrifuge. Excess supernatant was removed to obtain lipid pellets of 5-mm length, under argon. This standardized sample configuration was used in all conventional and saturation transfer ESR measurements (cf Fajer and Marsh, 1982; Hemminga et al., 1984). The samples were incubated at 50°C for 30 min, cooled to 15°C and kept at this temperature for 24 h before each experiment.

ESR spectroscopy

ESR spectra were recorded at a frequency of 9 GHz on an E-12 Century Line spectrometer (Varian Associates, Palo Alto, CA) equipped with nitrogen gas flow temperature regulation and interfaced to a PDP 11/10 (Digital Equipment Corporation, Waltham, MA) laboratory computer. Sample capillaries were centred in a standard 4-mm diameter quartz tube which contained light silicone oil for thermal stability. Conventional, first harmonic, in-phase, absorption spectra (V_1-display) were recorded at a modulation frequency of 100 kHz and modulation amplitude of 0.125 mT pp. STESR spectra were recorded in the second harmonic, 90° out-of-phase absorption mode (V'_2-display) at a modulation frequency of 50 kHz and a modulation amplitude of 0.5 mT pp. The phase was set by the self-null method (Marsh, 1981) at a subsaturating microwave field of 0.0032 mT. All STESR spectra were recorded with an average microwave field at the sample of $\langle B_1^2 \rangle^{1/2} = 0.025$ mT, according to a standardized protocol for dealing with cavity Q variations and field inhomogeneities (Fajer and Marsh, 1982; Hemminga et al., 1984). Details of the determination of $\langle B_1^2 \rangle^{1/2}$ and calibration of the spectrometer are described in Fajer and Marsh (1982). The normalized integral intensities of the STESR spectra were evaluated as described by Horváth and Marsh (1983).

RESULTS

Gel phase DPPC bilayers in water

The conventional ESR spectra of the 5-PCSL spin label in gel phase DPPC dispersions of increasing Ni^{2+} concentration are given in Fig. 1 and the corresponding saturation transfer ESR spectra are given in Fig. 2. The conventional ESR spectra change hardly at all in lineshape or intensity with Ni^{2+} concentration, indicating that the dipolar interactions are too weak to produce observable spectral broadening. The line shape of the saturation transfer ESR spectra also does not change very greatly with increasing Ni^{2+} concentration, as seen from the diagnostic line height ratios (see Thomas et al., 1976, for a definition) which are given in Fig. 3. Appreciable changes are found only in the central C'/C ratio.

In contrast to the diagnostic line-height ratios, the STESR integral intensity, I_{ST}, of the 5-PCSL spin label depends rather strongly on the concentration of paramagnetic ions, c_M, in the aqueous phase (See Fig. 4). The effects of paramagnetic ion-induced relaxation can be described by assuming that the intensity of the STESR spectrum is directly proportional to the spin-lattice relaxation time, T_1, as found by spectral simulations (Thomas et al., 1976), i.e.,

$$I_{ST} = I^0_{ST} \cdot T_1/T^0_1, \tag{1}$$

where I^0_{ST} and T^0_1 are the values of I_{ST} and T_1, respectively, in the absence of paramagnetic ions. This leads to the following dependence of the reciprocal STESR integral on paramagnetic ion concentration:

$$1/I_{ST} = (1/I^0_{ST})[1 + T^0_1 (dT^{-1}_{1M}/dc_M) \cdot c_M], \tag{2}$$

where T^{-1}_{1M} is the metal ion contribution to the T_1 relaxation rate of the spin label and is directly propor-

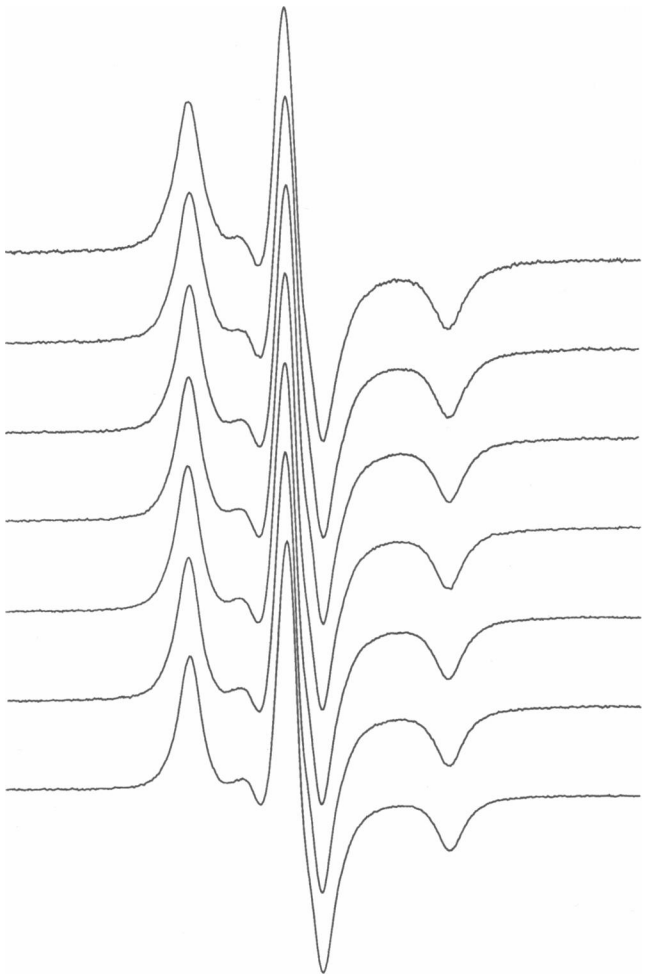

FIGURE 1 Conventional in-phase ESR spectra (V_1-display) of the 5-PCSL phosphatidylcholine spin label (0.5 mol%) in dispersions of dipalmitoyl phosphatidylcholine containing increasing concentrations of Ni^{2+}. From top to bottom: 2, 4, 8, 12, 15, 24, and 40 mM $NiCl_2$, respectively. Total scan width = 16 mT; T = 0°C.

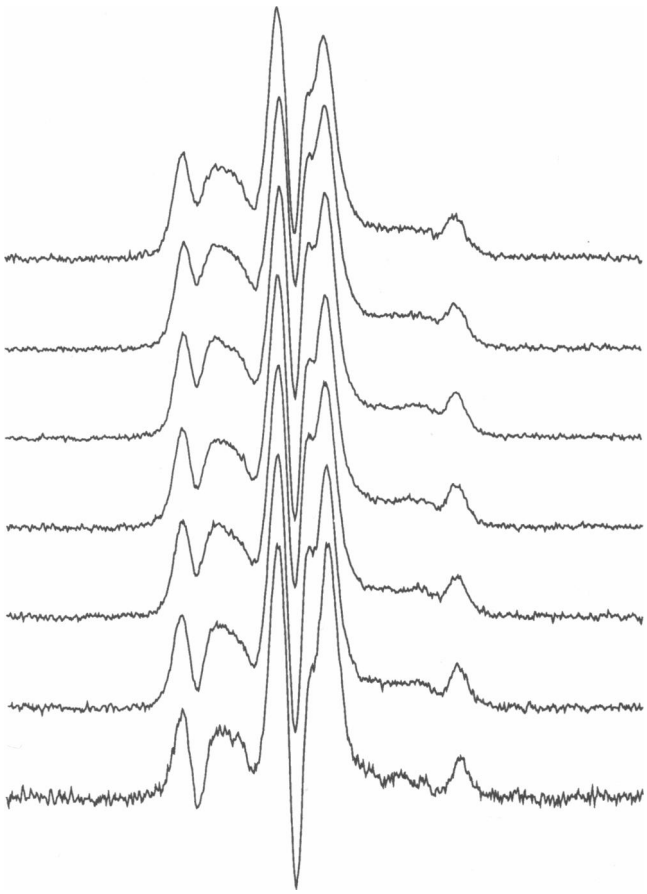

FIGURE 2 Second harmonic out-of-phase STESR spectra (V'_2-display) of 5-PCSL (0.5 mol%) in DPPC dispersions containing increasing concentrations of Ni^{2+}. From top to bottom: 2, 4, 8, 12, 15, 24, and 40 mM $NiCl_2$, respectively. Total scan width = 16 mT; T = 0°C.

tional to concentration. The linear dependence on Ni^{2+} ion concentration given in Eq. 2 is found for all the different spin labels, n-PCSL, as illustrated in Fig. 4 for 5-PCSL, hence, substantiating the assumption that I_{ST} is linearly proportional to T_1.

The gradient of the reciprocal STESR integral with Ni^{2+} ion concentration is given as a function of chain position, n, of the nitroxide group for the different n-PCSL phosphatidylcholine spin labels in gel phase bilayers of DPPC in Fig. 5. The profile shows a strong dependence of the paramagnetic ion-induced reduction in I_{ST} on the distance of the spin label group from the water phase containing the Ni^{2+} ions. The reduction in I_{ST} for nitroxides positioned closer to the aqueous interface is much greater than that for those situated at the centre of the bilayer.

INTERDIGITATED DPPC GEL PHASE IN GLYCEROL

Similar experiments have been performed for DPPC dispersed in glycerol which is known to induce a gel phase in which the lipid chains are interdigitated (McDaniel et al., 1983). The increases in $1/I_{ST}$ at 30 mM Ni^{2+} relative to the values in the absence of Ni^{2+} ions are given for the different spin labels in DPPC at 0°C, both in glycerol and in water media, in Fig. 6. The effect of chain interdigitation for the DPPC gel phase in glycerol is seen immediately by comparison with the profile with respect to chain position for DPPC in water. Instead of the characteristic decrease with increasing position down the chain seen in the bilayer structure, the profile is much shallower in the interdigitated phase. In the DPPC/glycerol system, the greatest reduction in I_{ST} is found for the 16-PCSL label at the end of the chain

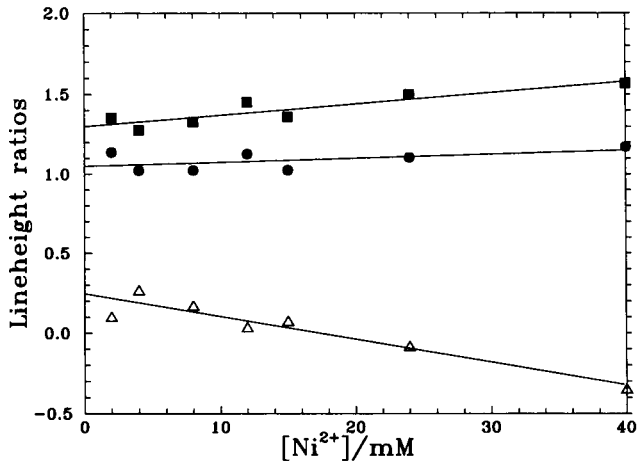

FIGURE 3 Dependence of the diagnostic line height ratios in the STESR spectra of 5-PCSL in aqueous DPPC dispersions on Ni^{2+} concentration. (■) low-field ratio, L''/L; (●) high-field ratio, H''/H; (△) central ratio, C'/C.

rather than for the 4-PCSL label close to the polar headgroup region, as is observed in DPPC/water dispersions.

DISCUSSION

The results presented here clearly indicates that saturation transfer ESR spectroscopy has sufficient sensitivity

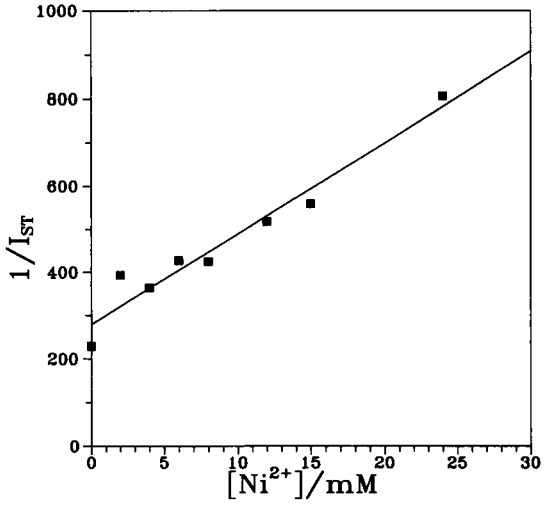

FIGURE 4 Dependence of the reciprocal saturation transfer integral, $1/I_{ST}$, of the 5-PCSL phosphatidylcholine spin label in dispersions of DPPC at 0°C on bulk Ni^{2+} concentration in the aqueous phase. The solid line represents a linear regression.

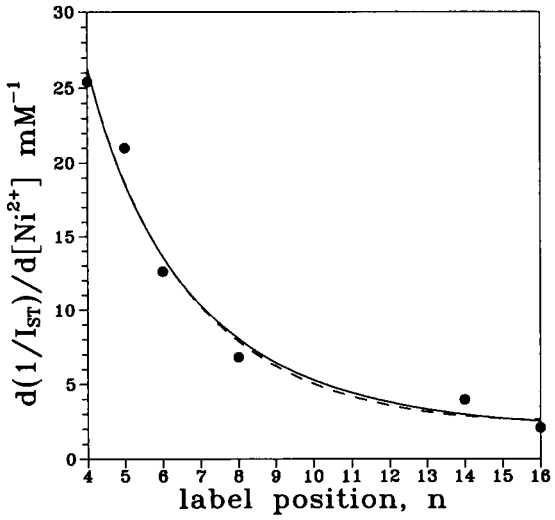

FIGURE 5 Dependence of the gradient of the reciprocal saturation transfer integral with respect to Ni^{2+} concentration, $d(1/I_{ST})/d[Ni^{2+}]$, on nitroxide position, n, in the sn-2 chain of n-PCSL phosphatidylcholine spin labels in aqueous DPPC dispersions at 0°C. The solid line represents a nonlinear least squares fit to Eq. 6 with $m = 3$ (parameters: $n_1 = 44.5$, $n_0 = 4.0$, $k'_3 = 13.1 \times 10^3\ mM^{-1}$), and the dashed line is the corresponding fit with $m = 4$ (parameters: $n_1 = 46.0$, $n_0 = 6.9$, $k'_4 = 37.0 \times 10^4\ mM^{-1}$).

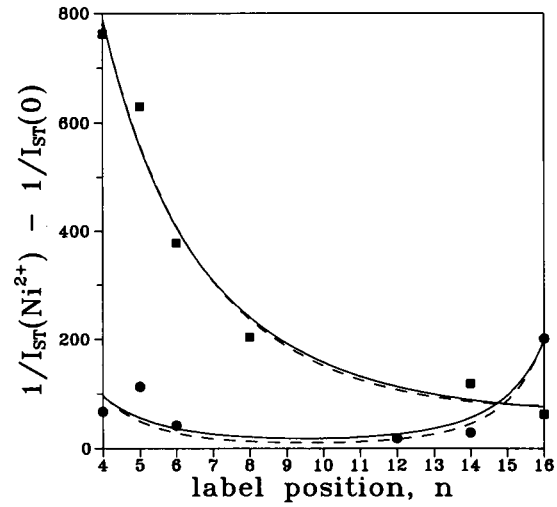

FIGURE 6 Dependence of the difference in reciprocal saturation transfer integral in the presence and absence of 30 mM Ni^{2+}, $1/I_{ST}(Ni^{2+}) - 1/I_{ST}(0)$, on nitroxide position, n, in the sn-2 chain of n-PCSL phosphatidylcholine spin labels in DPPC dispersions in glycerol (●) and in water (■) at 0°C. The solid lines represent nonlinear least squares fits to Eq. 6 with $m = 3$ (parameters: $n_1 = 20.5$, $n_0 = 0.75$, $k'_3 = 3.3 \times 10^2\ mM^{-1}$ for glycerol), and the dashed lines are the corresponding fits with $m = 4$ (parameters: $n_1 = 21.6$, $n_0 = 1.2$, $k'_4 = 2.4 \times 10^3\ mM^{-1}$ for glycerol).

to spin–spin interactions with paramagnetic ions for reliable determination of distance information in membranes and in biological systems generally. The distance dependence arises because the T_1 relaxation of the spin label by the paramagnetic ion is mediated by magnetic dipole–dipole interactions (cf Hyde et al., 1979). By use of spin labels located at defined positions in the lipid chains it is possible to calibrate the method without precise knowledge of the T_1 of the paramagnetic ion. This is done below from the measurements on gel phase lipid bilayers and used further to derive dimensional information on the interdigitated lipid gel phase in glycerol.

Dipolar paramagnetic relaxation

The spin-labeled lipid chains are immobilized in the gel phase with a well-defined position of the nitroxide group relative to the bilayer surface and the bilayers themselves are so large in area that they may be considered as essentially static. Therefore it seems likely that a solid-state mechanism for the dipolar relaxation is the most appropriate. The alternative possibility of relaxation induced by modulation of the dipolar interaction due to translational diffusion of the mobile paramagnetic ions is considered later and rejected.

The solid-state mechanism for dipolar-induced spin-lattice relaxation has a $1/r^6$ dependence on the separation between dipoles (see, e.g., Hyde et al., 1979). Summing over all metal ions then gives the following expression for the total dipolar-induced relaxation rate:

$$1/T_{1M} = \sum_k f(\Theta_k)/r_k^6, \qquad (3)$$

where r_k is the distance of the kth paramagnetic ion from the spin-label center and Θ_k is the angle between the interdipole vector and the static magnetic field direction. The function $f(\Theta_k)$ also depends on the T_1 of the paramagnetic ion and the resonance frequencies of spin label and paramagnetic ion, all of which remain constant in the present situation. Integrating over all paramagnetic ions on one side of the bilayer then yields the following for the paramagnetic ion-induced relaxation rate:

$$1/T_{1M} = f^0 c_M \int d\tau/r^6 = f_m \cdot c_M/R^m, \qquad (4)$$

where R is the distance of the spin label from the bilayer surface, and f^0 and f_m are constants that, in principle, depend on the orientation, Θ, of the static magnetic field relative to the bilayer normal. A value of $m = 3$ is obtained by integrating over all space on one side of the bilayer. If the angular dependences are neglected, because to a first approximation they are insignificant compared with the $1/r^6$ dependence (cf Hyde et al., 1979), then $f_3/f^0 = \pi/6$. On the other hand, integration over a narrow layer of paramagnetic ions absorbed at the bilayer surface would yield a value of $m = 4$ with $f_4/f^0 = K\pi/2$, if the angular dependences are neglected, where K is effectively a surface binding constant.

Substituting Eq. 4 in Eq. 2 yields the following dependence of the STESR integral on the paramagnetic ion concentration and distance of the spin label from the bilayer surface:

$$1/I_{ST} = 1/I_{ST}^0 + k_m[R^{-m} + (d_l - R)^{-m}]c_M, \qquad (5)$$

where d_l is the total bilayer thickness, $m = 3$ or 4, and if the angular dependences are neglected then $k_m = (T_1^0/I_{ST}^0)f_m$. The two separation-dependent terms in Eq. 5 allow for both sides of the bilayer. Expressing the distances appearing in Eq. 5 in terms of equivalent CH_2 units of the lipid chain gives the following expression for the paramagnetic ion concentration dependence of $1/I_{ST}$ as a function of the spin label chain position, n:

$$d(1/I_{ST})/dc_M = k'_m[(n_0 + n)^{-m} + (n_l - n_0 - n)^{-m}], \qquad (6)$$

where n_0 is the effective distance in CH_2 units of the bilayer surface from the origin of the numbering of the *sn*-2 chain labeling, n_l is the bilayer thickness in CH_2 units and $k'_m = (dR/dn)^{-m}k_m$. The gradients of the concentration dependence of $1/I_{ST}$ for the different positional isomers of the *n*-PCSL spin label in gel phase DPPC bilayers at 0°C were given above in Fig. 5. To within the experimental accuracy, the positional dependence is well described by Eq. 6, giving support for the solid state dipolar mechanism.

Gel phase bilayers in water

A nonlinear least squares fit of the data in Fig. 5 to Eq. 6 with $m = 3$ yields values of $n_l = 44.5$ and $n_0 = 4.0$ (CH_2 units). Allowing for a mean chain tilt of $\Theta = 35^0$ in the L_β', phase (Janiak et al., 1976), the value of n_l corresponds to a bilayer thickness of $d_l = 1.27$ (Å) $\cos\Theta \cdot n_l =$ 46 Å. This is in good agreement with the results of x-ray diffraction from which a bilayer thickness of 47 Å has been obtained for DPPC at 10°C (Janiak et al., 1976). Two extra CH_2 units must be added to the value of n_0 to obtain the equivalent thickness of the lipid polar group region, because of the bent configuration of the *sn*-2 chain (Seelig and Seelig, 1980; Pearson and Pascher, 1979). Allowing again for the chain tilt, then yields a value of $d_p = 6$ Å for the thickness of the polar group. For comparison, a corresponding value of 7.3 Å is found in the x-ray crystal structure of lauroyl propanediol-phosphocholine with tilted chains and of 10.4 Å in the

less tilted structure of crystalline dimyristoyl phosphatidylcholine (Hauser et al., 1981).

The above considerations (with $m = 3$) have made no allowance for the multibilayer nature of the lipid dispersions. If this is done, the quantity given in square brackets in Eq. 5 should be replaced by the expression:

$$f(R, d_l, d_w) = \sum_{j=0}^{i=1} [(R + r_j)^{-3} + (d_l - R + r_j)^{-3} - (R + r_j + d_w)^{-3} - (d_l - R + r_j + d_w)^{-3}] + [(R + r_i)^{-3} + (d_l - R + r_i)^{-3}]d_w/(d_w + d_l), \quad (7)$$

where d_w is the thickness of the water layers between the bilayers and $r_j = j(d_l + d_w)$ with j being the index for the different layers extending out from the central lipid layer. In Eq. 7 the multibilayers are considered to be of infinite extent and from $j = i$ outwards are treated as a continuum with average paramagnetic ion density proportional to $d_w/(d_w + d_l)$. A fit of comparable quality to that for $m = 3$ in Fig. 5 can be obtained using the version of Eq. 6 corresponding to the expression given in Eq. 7. However, there are then four free parameters to be determined by the six data points. In addition, the values of d_w must be restricted to a realistic range, because it is already shown in Fig. 5 that a good fit can be obtained when d_w is allowed to go to infinity. With these restrictions and taking $i = 2$, the following bilayer dimensions are obtained from the fitting parameters: $d_l = 44$ Å, $d_p = 6.5$ Å and $d_w = 15$ Å. The values for d_l and d_p are comparable to those obtained in the previous fit and the value of d_w is in good agreement with the water layer thickness of 16 Å obtained for DPPC at 10°C by x-ray diffraction (Janiak et al., 1976).

It may be considered why the model that does not take account of the multibilayer structure of the lipid dispersions provides reasonable fits to the positional dependence that also yield realistic estimates for the bilayer dimensions. One reason probably lies in the short-range nature of the $1/r^6$ dependence. A further reason could be that the parameter k'_3 in Eq. 6 with $m = 3$ effectively scales the paramagnetic ion concentration in a manner similar (but not identical) to the factor in the last term of Eq. 7. In fact, a value of $k'_3 = 14.8 \times 10^3$ mM^{-1} is obtained for the fit to the multilayer model, which is quite close to that obtained from the fit to Eq. 6 with $m = 3$. This latter result suggests that the value obtained here for $k_3 \approx 15.7 \times 10^3$ Å$^3 \cdot$ mM^{-1} might be used, with appropriate adjustment for the value of f_3/f^0, as a first approximation in deriving distance information from saturation transfer integral measurements on other systems with different geometries. The assumption made in such an approach is that the angular factors are much less important than the $1/r^6$ dependence in determining the dipolar relaxation (cf Hyde et al., 1979).

It is appropriate to check whether the value obtained for k_3 by fitting the STESR data is of a reasonable order of magnitude for a dipolar relaxation mechanism. In the limit of fast metal ion relaxation, the Solomon-Bloembergen equation yields the following approximation for the effective value of f^0 in spherically symmetrical systems (see, e.g., Dwek, 1973; Bertini and Luchinat, 1986):

$$f^0 = (4/3)\, g_{pm}^2 \beta^2 S(S + 1)\gamma^2 T_{1pm} N_A \cdot 10^{-3}, \quad (8)$$

where γ is the gyromagnetic ratio of the spin label; g_{pm}, S and T_{1pm} are the g-value, spin and T_1 relaxation time, respectively, of the paramagnetic ion; β is the Bohr magneton and N_A is Avogadro's number. Taking $g_{pm} = 2.25$ and $S = 1$ for the hexa-aquo Ni^{2+} complex and a mean value of $T_1^0/I_{ST}^0 = 7\times10^{-3}$ s for the spin label (Fajer et al., 1992), this approximation leads to an estimate of $T_{1pm} = 2\times10^{-11}$ s from the above value of k_3. Spin-lattice relaxation times for hexa-aquo Ni^{2+} are expected to be somewhat shorter than this value, which lies at the upper end of the range deduced from NMR relaxation enhancements (Bertini and Luchinat, 1986). It is possible that the estimate may be somewhat affected by the assumption of fast metal ion relaxation. Additionally, there are uncertainties in the above approximation due to the different geometry in the bilayer system. Nonetheless, this estimate suggests that the value deduced for k_3 lies within a range that is not unreasonable for a dipolar mechanism.

Some preferential adsorption of divalent ions (other than Ni^{2+}) to DPPC polar headgroups has been found previously (Lis et al., 1981). It is therefore of interest to investigate to what extent the Ni^{2+}-induced relaxation may be interpreted in terms of a layer of absorbed paramagnetic ions. From Fig. 5, it is seen that the positional dependence may also be fit to Eq. 6 with the exponent $m = 4$. The parameters derived for the bilayer dimensions are: $n_l = 46$ and $n_0 = 6.9$, corresponding to $d_l = 48$ Å and $d_p = 9$ Å, respectively. The higher value of d_p suggests that surface absorption may play some part in determining the relaxation induced by Ni^{2+}, because the value derived neglecting surface absorption is somewhat lower than that obtained by x-ray diffraction. However, surface adsorption is unlikely to give the major contribution to the relaxation, because the binding of divalent ions to DPPC headgroups is relatively weak.

Interdigitated gel phase in glycerol

The profile of the Ni^{2+}-induced reduction in I_{ST} for the chain-labeled lipids given in Fig. 6 indicates that the chain interdigitation in the presence of glycerol is almost

complete. The lipid chains overlap fully since 16-PCSL is relaxed more efficiently by Ni^{2+} ions in the glycerol phase than is 4-PCSL. The expression given in Eq. 6 for the dependence of the saturation transfer integral on spin label position and lipid layer thickness is also valid for interdigitated lipid phases. Although there is more scatter in the data for DPPC in glycerol, because of greater spin–spin interactions between labels in this system, the positional dependence of the relaxation rate can be described reasonably well by Eq. 6. Extrapolation of the theoretical curve in Fig. 6 indicates that the nitroxide of 16-PCSL is located in the region of the C-3 atom in the *sn*-2 chain of the oppositely oriented phospholipid molecule. This implies that the terminal methyl groups on opposite sides of the lipid layer are separated by $\sim 13 \times 1.27$ Å = 16.5 Å. Previous data from x-ray diffraction were unable to define so precisely the degree of chain interdigitation, yielding a separation of the methyl groups of in the region of 12 Å (McDaniel et al., 1983.)

The interdigitated nature of the DPPC phase in glycerol is also clear from the symmetry of the profile deduced from Eq. 6. For $m = 3$, this profile is characterized by values of $n_l = 20.5$ and $n_0 = 0.75$ (CH_2 units). The effective thickness of the DPPC lipid layer in glycerol is therefore ~60% of that of DPPC in water, assuming that the chains are untilted in the interdigitated phase. This reduction is somewhat greater than that observed by x-ray diffraction (McDaniel et al., 1983), because the Ni^{2+} ions are able to penetrate beyond the lipid polar headgroups to come into closer contact with the chain ends. Taking a polar group thickness of 6 Å (cf above) and volume of 340 $Å^3$ (Tardieu et al., 1973), yields an area occupied by the polar group itself of only 57 $Å^2$ as opposed to the total surface area per polar group of 79.3 $Å^2$ (McDaniel et al., 1983) in the interdigitated phase. Again, allowing for the bend in the *sn*-2 chain, the effective thickness of the lipid polar group in glycerol is ~60% of that in water. This reduction corresponds to the much larger surface area per molecule in the interdigitated phase which allows the polar group to relax fully parallel to the lipid surface and also allows greater accessibility of the Ni^{2+} ions to the spin labels at the polar head-group end of the chains. In these cases also, the STESR relaxation data are able to augment the structural definition obtained from x-ray diffraction.

Again, a fit of comparable quality can be obtained also for the model with $m = 4$. The parameters derived for DPPC in glycerol are: $n_l = 21.6$ and $n_0 = 1.2$ (CH_2 groups). Compared with the data for DPPC in water, these values correspond to a 40% thinning in the effective thickness of the lipid layer and a 55% thinning in the polar group region. Thus, irrespective of the mode of analysis, the relaxation studies provide a clear indication of the chain interdigitation and yield reasonable estimates for the thickness of the lipid layer.

Diffusional dipolar relaxation mechanism

Finally, it may be enquired whether a liquid state (i.e., diffusional) model, rather than a solid-state model, might be appropriate for describing the dipolar relaxation. The dipolar correlation time in the liquid state mechanism is $\tau_d = d^2/D_T$, where d is the distance of closest approach and D_T is the translational diffusion coefficient, which is inversely proportional to the solvent viscosity (Abragam, 1961). In the limit of fast diffusion relative to the paramagnetic ion relaxation rate (and relative to the resonance frequency), the spin label relaxation rate should be proportional to the solvent viscosity, independent of the paramagnetic ion T_1 and inversely proportional to the distance of closest approach of the dipoles (cf Pfeifer, 1961; Abragam, 1961). The large reduction in the Ni^{2+}-induced relaxation rate for labels closer to the polar headgroups in the presence of glycerol relative to that in water (see Fig. 6) and the pronounced dependence on the distance of closest approach in water therefore argues against a diffusional mechanism. (The decreased relaxation rate of 4-PCSL in glycerol compared with that in water is most probably due to a change in the intrinsic spin-lattice relaxation time of the paramagnetic ion in glycerol relative to the hexa-aquo complex. An approximate value of $T_{1pm} = 6.10^{-13}$ s in glycerol is estimated using the methods outlined above.) For intermediate rates of diffusion, it is likely that the relaxation rate would also have a low dimensionality in the distance of closest approach (Pfeifer, 1961; 1963). An inverse square relation gives a substantially worse fit to the positional dependence of the relaxation rate in water than those in Fig. 5 and hence may be discounted. In the limit of very slow diffusion, a $1/R^3$ dependence is obtained and the mechanism goes over to that for solid state systems which is the more compatible with the experimental data, as shown above.

Conclusions

In summary, the relaxation experiments with Ni^{2+} ions give a pronounced dependence on the position of the spin-label group in the bilayer that is characteristic of a solid-state dipolar mechanism. Values may then be derived for the lipid bilayer dimensions that are consistent with the results of x-ray diffraction. Further confirmation is given by the unambiguous detection of lipid chain interdigitation in glycerol, which serves to delineate further the nature of the interdigitated phase.

Saturation transfer ESR is established as a viable method for determining spin-label locations in biological systems and the calibration provided here on lipid systems can be applied generally to distance measurements in aqueous systems containing Ni^{2+} ions.

Tibor Páli thanks the Federation of European Biochemical Societies for the award of a long-term fellowship.

Received for publication 9 September 1991 and in final form 12 February 1992.

REFERENCES

Abragam, A. 1961. The Principles of Nuclear Magnetism. Oxford University Press, Oxford. 599 pp.

Bertini, I., and C. Luchinat. 1986. NMR of Paramagnetic Molecules in Biological Systems. Benjamin/Cummings, Menlo Park, CA. 319 pp.

Dwek, R. A. 1973. Nuclear Magnetic Resonance in Biochemistry. Oxford University Press, Oxford. 395 pp.

Fajer, P., and D. Marsh. 1982. Microwave and modulation field inhomogeneities and the effect of cavity Q in saturation transfer EPR spectra. Dependence on sample size. *J. Magn. Reson.* 49:212–224.

Fajer, P., A. Watts, and D. Marsh. 1992. Saturation transfer, continuous wave saturation and saturation recovery electron spin resonance studies of chain-spin labeled phosphatidylcholines in the low temperature phases of dipalmitoyl phosphatidylcholine bilayers. The effects of rotational dynamics and spin–spin interactions. *Biophys. J.* 61:000–000.

Hauser, H., I. Pascher, R. H. Pearson, and S. Sundell. 1981. Preferred conformation and molecular packing of phosphatidylethanolamine and phosphatidylcholine. *Biochim. Biophys. Acta.* 650:21–51.

Hemminga, M. A., P. A. de Jager, D. Marsh, and P. Fajer. 1984. Standard conditions for the measurement of saturation transfer ESR spectra. *J. Magn. Reson.* 59:160–163.

Horváth, L. I., and D. Marsh. 1983. Analysis of multicomponent saturation transfer EPR spectra using the integral method: application to membrane systems. *J. Magn. Reson.* 54:363–373.

Horváth, L. I., L. Dux, H. O. Hankovszky, K. Hideg, and D. Marsh. 1990. Saturation transfer electron spin resonance of Ca^{2+}-ATPase covalently spin-labeled with β-substituted vinyl ketone- and maleimide-nitroxide derivatives. Effects of segmental motions and spin–spin interactions. *Biophys. J.* 58:231–241.

Hyde, J. S., H. M. Swartz, W. E. Antholine. 1979. The spin-probe-spin label method. *In* Spin Labelling II. Theory and Applications. L. J. Berliner, editor. Academic Press, New York. 71–113.

Janiak, M. J., D. M. Small, and G. G. Shipley. 1976. Nature of the thermal pretransition of synthetic phospholipids: dimyristoyl- and dipalmitoyllecithin. *Biochemistry.* 15:4575–4580.

Khramtsov, V. V., and D. Marsh. 1991. Measurement of the local translational diffusion rates of proteins by saturation transfer EPR spectroscopy. *Biochim. Biophys. Acta.* 1068:257–260.

Likhtenshtein, G. I. 1976. Spin Labeling Methods in Molecular Biology. Wiley-Interscience, New York. 258 pp.

Likhtenshtein, G. I. 1990. Nitroxides in the solution of some problems of chemical biophysics. *Pure Appl. Chem.* 62:281–288.

Lis, L. J., W. T. Lis, V. A. Parsegian, and R. P. Rand. 1981. Adsorption of divalent cations to a variety of phosphatidylcholine bilayers. *Biochemistry.* 20:1771–1777.

Marsh, D. 1981. Electron spin resonance: spin labels. *In* Membrane Spectroscopy. E. Grell, editor. Springer-Verlag, Berlin, Heidelberg. 51–142.

Marsh, D., and A. Watts. 1982. Spin labeling and lipid-protein interactions in membranes. *In* Lipid-Protein Interactions. Vol. 2. P.C. Jost and O. H. Griffith, editors. Wiley-Interscience, New York. 53–126.

Marsh, D., and L. I. Horváth. 1992. Influence of Heisenberg spin exchange on conventional and phase quadrature EPR lineshapes and intensities under saturation. *J. Magn. Reson.* 97:13–26.

McDaniel, R., T. McIntosh, and S. Simon. 1983. Nonelectrolyte substitution for water in phosphatidylcholine bilayers. *Biochim. Biophys. Acta.* 731:97–108.

Pearson, R. H., and I. Pascher. 1979. The molecular structure of lecithin dihydrate. *Nature (Lond.).* 281:499–501.

Pfeifer, H. 1961. Der Translationsanteil der Protonrelaxation in wäßrigen Lösungen paramagnetischer Ionen. *Ann. Physik.* 8:1–8.

Pfeifer, H. 1963. Zur kernmagnetischen Relaxation der Wasserprotonen in wäßrigen Lösungen paramagnetischer Macromoleküle. *Biochim. Biophys. Acta.* 66:434–439.

Seelig, J., and A. Seelig. 1980. Lipid conformation in model membranes and biological membranes. *Q. Rev. Biophys.* 13:19–61.

Tardieu, A., V. Luzzati, and F. C. Reman. 1973. Structure and polymorphism of the hydrocarbon chains of lipids: a study of lecithin-water phases. *J. Mol. Biol.* 75:711–733.

Thomas, D. D., L. R. Dalton, and J. S. Hyde. 1976. Rotational diffusion studied by passage saturation transfer electron paramagnetic resonance. *J. Chem. Phys.* 65:3006–3024.